Isotopic product distributions in the near symmetric mass region in proton induced fission of ^{238}U

P. P. Jauho, A. Jokinen, M. Leino, J. M. Parmonen, H. Penttilä,* and J. Äystö
Department of Physics, University of Jyväskylä, FIN-40351 Jyväskylä, Finland

K. Eskola
Department of Physics, University of Helsinki, FIN-00170 Helsinki, Finland

V. A. Rubchenya
V. G. Khlopin Radium Institute, St. Petersburg-194021, Russia
(Received 4 November 1993)

We have studied fission product yields using 19.8 MeV proton induced fission of a thin ^{238}U target and the on-line mass separator IGISOL. The nonselectivity of the separation method used with respect to Z has allowed accurate determination of the yields of symmetric fission for the first time. The cumulative yields for the elements from $Z = 40$ (Zr) up to $Z = 47$ (Ag) have been determined from the beta- and gamma-radioactivity measurements. The independent fission product yield distributions for elements Tc, Ru, and Rh are obtained from the experimental data. An improved theoretical model for calculating mass and independent yields is described and applied. It is found that the charge splitting for the primary fragments differs from that obtained with the unchanged charge division model at moderate excitation energies of compound nuclei. A comparison of the calculated and experimental fission product yields shows that the model presented can be applied for predictions of cross sections for very neutron-rich nuclei in the light particle induced fission.

PACS number(s): 25.85.Ge, 24.10.−i, 23.20.−g, 23.40.−s

I. INTRODUCTION

There are only few mass and charge distributions measured with on-line mass separators for a nearly symmetric mass division of fission products [1–3]. However, there are some studies of cumulative mass distributions taking advantage of gamma spectroscopy without mass separation [4,5]. The ion guide isotope separation technique IGISOL, employed in this work, is fast and allows direct determination of both independent and cumulative yields of nuclei on the neutron rich side of the isotopic fission product distribution. Moreover, when using thermal-neutron-induced fission and spontaneous fission one cannot reliably determine nuclear charge and mass dispersion parameters for symmetric products because of their low production rates. As more energy is brought into the system, for instance, by charged particles, the symmetric component in the mass distribution is enhanced [6].

In this paper we continue our study of isotopic distributions initiated in Ref. [1], in which we measured charge dispersion for the mass chains $A = 110$, 112, 114, and presented preliminary cumulative isotopic distributions for elements ranging from Tc to Ag. These experiments were carried out in the mass region $A = 108$–120 using 20 MeV protons and a set of four, 20 mg/cm^2, ^{238}U targets. In this paper we use only one target in the setup to define the excitation energy better and to allow larger opening angle of fission fragments to be captured by the ion guide system. Moreover, a significant improvement on the knowledge of the decay schemes of nuclei of interest has been obtained recently, largely due to the experimental work at the IGISOL facility. This allows now a more reliable extraction of the yields than before. The covered mass region $A = 96$–120 is broader than in our earlier experiment and allows us to compare yields in the asymmetric and symmetric mass region not only by mass but also isotopicwise.

Ion guide based on-line mass separation technique is ideally suited for the measurements of the broad isotopic distributions. It has a very short delay time of a few ms, independent of Z of the nuclide. Hence, it covers the shortest possible beta-decay half-lives of fission products. The radioactive ion beam implanted at the counter position is free from decay products, only primary product ions are separated and corrections for the radioactive decays are minimized. The transmission efficiency of the technique is not absolutely independent of Z, but small deviations due to slightly different ionic recombination probabilities as well as chemical reactions exist. For these reasons, high precision measurements on yields are possible only for isotope chains.

Present work was undertaken to study the parameters of the isotopic distributions and to obtain information on the charge-division mechanism, on competition between different fission modes and on influence of pre- and post-

*Present address: Argonne National Laboratory, Argonne, IL 60439.

fission neutron emission. The deduced parameters: the average mass, the width, and the asymmetry parameter are of importance for prediction of the yields of very neutron-rich nuclei. The experimental results are analyzed in the framework of the theoretical model introduced in Ref. [5] and used here in a more advanced form. In the present form the model includes consideration of different chances for fission, a new approach in the systematics of fission product yields and inclusion of shell effects in neutron emission process. The results of the calculations of the mass yields and the isotopic fission product distribution and their comparison with experimental results are presented in this paper.

II. EXPERIMENTAL METHOD

Present experiments used the 10.0 mg/cm^2 natural U target which is basically composed of ^{238}U. The maximum energy of the MC-20 cyclotron, used in this work, was 20 MeV for protons with typical intensities of 0.5–1 μA. The IGISOL facility [7,8] was used to separate nuclides belonging to the mass chain of interest from other fission products. The U target was covered with a 0.2 mg/cm^2 Al foil on both sides. A 0.9 mg/cm^2 Ni foil separated the target chamber from the thermalizing gas cell of the IGISOL system, as shown in Fig. 1. Radioactive ions thermalized in 100 mbar helium attain an electric charge of +1 and are extracted by gas flow through a differentially pumped electrode system for acceleration to 40 keV. The accelerated ions are then separated according to their mass in the 55° dipole magnet with a bending radius of 1.5 m. The mass resolving power of the system, $M/\Delta M$, was typically about 400. More details of the method used can be found in Ref. [8].

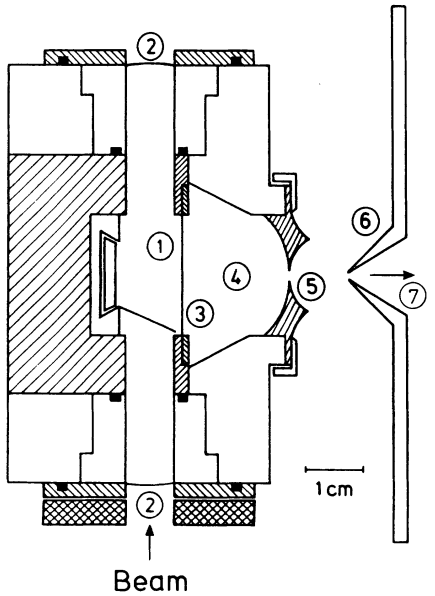

FIG. 1. Experimental setup of the target system and the ion guide. (1) Uranium target, (2) beam windows, (3) nickel foil, (4) stopping chamber, (5) exit aperture, (6) skimmer electrode, (7) singly charged fission product ions.

Beams of fission product ions were implanted on a 0.6 cm wide collector tape, which was directly viewed by a set of beta- and gamma-ray detectors. The yield of a specific isotope was extracted from the measured radioactivity after corrections for the detection efficiency and the branching of the observed γ transitions. The production rate was then obtained by dividing the yield with the integrated beam current. The counting setup composed of a 50% Ge detector, a planar 10 mm thick Ge x-ray detector, and a 1 mm thick plastic ΔE detector positioned in front of the large Ge detector. The size and the position of the separator beam spot was well defined and the distance of it from the γ detector was kept as 7 mm. Typically the β-coincident gamma-ray spectra were recorded with both Ge detectors and in some cases also low energy singles gamma spectra were useful. In the peak analysis an automatic peak search procedure was used [9]. Typically, the spectra were recorded in saturation mode, i.e., without moving the activity from the counting position. Measuring times varied from 0.5 to 4 hours per mass number. As an example, we give in Fig. 2 a spectrum taken at mass $A = 114$, which demonstrates the sensitivity of our technique; evidence of isobars with $Z = 44$, 45, 46, and 47 can be seen in the spectrum.

Scanning of the wide mass range, $A = 96$–120, required stable operation of the system. The beam in the MC-20 cyclotron was stable only to ±25%. For this reason, the integrated beam current was determined using the $\gamma(\beta)$ yield. A TDC (time to digital converter) unit gave a time of occurrence label on each $\gamma(\beta)$ event. One projection of the events was showing constantly the total time profile of the TDC or the counting rate, which effectively monitored both the separator and the cyclotron beam operation. The cyclotron beam current was measured several times during each run and so we could compare the total counting rate and the cyclotron beam current at these times.

III. EFFECT OF ENERGY AND ANGULAR DISTRIBUTION OF FRAGMENTS ON THE OBSERVED YIELDS

Two fission fragments are created with a total kinetic energy TKE which the lighter fragment shares with the heavier one. The initial kinetic energy of a fragment depends on its mass A according to the simple relation $E = (239 - \nu_{\rm pre} - A)/(239 - \nu_{\rm pre})$TKE, where $\nu_{\rm pre}$ is the prefission neutron multiplicity and TKE=176.7 MeV [10]. To be accurate the TKE=TKE(A_L, A_H) is slightly dependent on the fragment masses. Prompt neutron and γ emission of the fragments do not appreciably alter the kinetic energy and angular distributions of the fission fragments.

Due to the large initial energy only a small fraction of fission fragments, i.e., about 1%, are stopped in helium in our set up. According to Northcliffe and Schilling [11] only fragments with energy below about 350 keV are stopped at a helium pressure of 100 mbar within the volume of the thermalizing chamber shown in Fig. 1. This necessitated the use of a thick target approach. The ini-

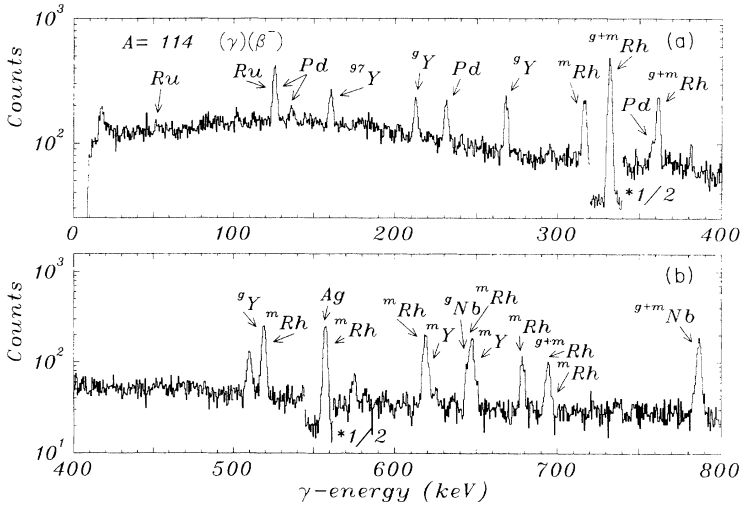

FIG. 2. A spectrum recorded at mass number $A = 114$. The activities observed are denoted by their chemical symbol.

tial position of the fragments produced in the target and stopped in helium, as well as of those with higher final energy, were calculated with the modified TRIM computer program [8,12] which utilizes Monte Carlo simulation. It was assumed that the fragments (A, Z, E) are produced uniformly throughout the target with an isotropic angular distribution. Due to the effect of the multiple scattering, mainly in the target itself, the distributions showed to be broader the smaller the final energies of the fragments are. For those ions, whose final energy was below 350 keV, the initial site distribution was practically constant from the surface to the back of the target. Taking into account that the ions had lost about 100 MeV in collisions inside the target we can assume that the setup accepts all initial scattering angles with equal weights. Thus a preferred scattering angle in fission as a function of fragment mass had no chance to interfere with our observations in the experiment.

The fraction of ions stopped in helium compared to the number of incident products in fission was calculated with the same TRIM program for six fission fragments (A, Z, E) covering the mass window $A = 96$–120. The probability of surviving of fragments from the target and through the Al and Ni foils into helium was found to be practically independent on the mass A and the nuclear charge Z. A critical judgment of the absolute accuracy of the TRIM calculation in this rather extreme special case is very difficult and experimental verification of the results is not possible in practice. However, only relative differences are important and were found to be insignificant. In particular, the effect of the actual TKE distribution was found to be small.

The anisotropy $W(0°)/W(90°)$ of the initial angular distribution $W(\theta)$ of a fragment with respect to the beam axis, varies as a function of the fragment mass from 1.0 to 1.4 being at its minimum for symmetric mass division in the case of low energy proton induced fission of uranium [13]. It means that both light and heavy products are favored at the $\theta = 0°$ scattering angle as compared to symmetric mass division. The geometry in our experimental setup favored slightly the $\theta = 90°$ emission angle and hence the symmetric mass division. However, multiple collisions of fission fragments in slowing down to low energy in the thick ^{238}U target smooth out the angular distribution as described above.

IV. RESULTS

Identification of the γ peaks was based on our earlier work with IGISOL [14–27] and on the available literature, mainly included in Nuclear Data Sheets. The intensities of all the observed γ peaks following the β decay of a particular nucleus were included in the isotope yield analysis. In the calculation of independent as well as cumulative yields the determination varied from nuclide to nuclide. In some cases nuclear structure considerations exclude the existence of a strong ground state branch [1]. The yields of isomers and their decay modes were considered. In this work we used continuous cyclotron and separator beams so nuclide identification based on half-life was not possible, but the yields were corrected according to half-life whenever necessary. Actually, recording decay events after the irradiation was performed in some cases. If the highest observed Z for a given mass number is significantly above the average Z we get a good estimate for the mass yield without any significant model-dependent corrections due to the charge distribution.

Cumulative mass yields measured with a single ^{238}U target using proton energy of 19.8 MeV together with the calculated values are shown in Fig. 3. The yield of the nuclide with the highest observed Z in each mass number was taken as an approximation to the total cumulative yield. These nuclides were ^{99,100}Nb, ^{104,105,106}Tc, ^{108,109,110,111,112}Rh, and ^{115,116,117,118}Ag. In this procedure the Z of the measured nuclide had to be higher than the most probable Z of the charge distribution of the isobar. If this condition was not fulfilled we marked the value as a lower limit for the total cumulative yield. The oxide yields of the ions produced as oxides have been added to the yields of the atomic ions. The elements from Y to Tc have been observed to form oxides in the system [8]. For this reason, a liquid nitrogen cooled activated

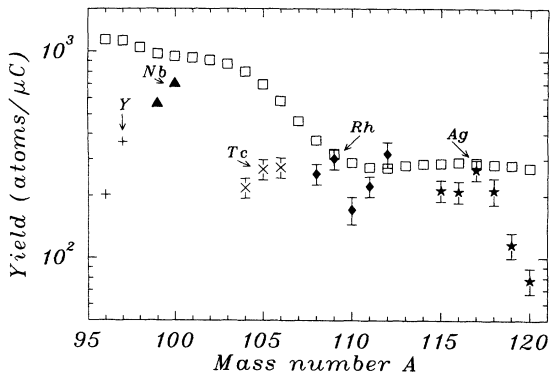

FIG. 3. Cumulative mass yields near the symmetric fission for 19.8 MeV p+^{238}U. The theoretical points are calculated as described in Sec. V. The experimental points are from Table I.

charcoal trap was used in all experiments to increase the purity of helium and reduce the oxide formation. A comparison of the experimental data of Fig. 3 with the data of Ref. [5] shows that there is a slight dependence of the efficiency of the separated elements on Z. Within the elements studied this efficiency fluctuation is less than a factor of 2.

Cumulative isotopic yields are given in Table I for Y, Zr, Nb, Mo, Tc, Ru, Rh, and Ag. The yields for Nb and Pd isotopes could not be extracted due to the lack of knowledge about the absolute beta branching ratios of several isotopes. For this reason, the independent isotopic yields could be extracted only for Tc, Ru, and Rh. They will be discussed later. The yields are given in atoms/s normalized to the beam current of 1 μA. Typically the intensity of the beam was between 0.5 and 1 μA. The variation of the beam intensity did not have any observable effect on the efficiency of the separator.

V. THEORETICAL MODEL

Here we will describe the theoretical model used in our calculation of independent and cumulative fission product cross sections in light particle-induced fission of heavy nuclei. This model was first described in Ref. [5]. In the following we introduce some improvements to the original version. To describe the probabilities of fission product formation in particle-induced fission there is a need to consider a few more physical effects important in the fission process.

(1) Emission of the prefission light particles and con-

TABLE I. Cumulative fission yields of isotopes for the elements with Z = 39–47 as measured at the focal point of the IGISOL separator in units of atoms/μC using the reaction 19.8 MeV p+^{238}U. The errors in parentheses include 10% uncertainty in the efficiency calibration and the statistical error. The values given inside brackets are lower limits only due to the uncertainty in the branching ratio.

A	Y(Z = 39)	Zr(Z = 40)	Nb(Z = 41)	Mo(Z = 42)	Tc(Z = 43)	Ru(Z = 44)	Rh(Z = 45)	Ag(Z = 47)
96	201							
97	365							
98								
99		387(42)	561					
100		483(53)	699					
101		264(35)						
102		198(23)						
103		[18.2(23)]						
104		35(7)		173(24)	218(24)			
105				162(25)	268(30)			
106				115(14)	274(31)			
107				26.6(32)	220(25)	220(26)		
108					163(19)	177(20)	255(29)	
109					91(11)	[55.9(67)]	303(35)	
110					34.5(42)	104(13)	171(26)	
111					[1.66(29)]	94(12)	222(25)	
112					3.08(52)	100(12)	319(45)	
113						19.9(26)	132(16)	[298(36)]
114							119(15)	[462(57)]
115							24.1(39)	213(25)
116							20.3(31)	210(25)
117								267(30)
118								212(31)
119								116(16)
120								78(11)

tributions of different fission channels.

(2) Attenuation of nuclear shell effects with increasing excitation energy of compound nuclei which leads to changes in the relative yields of symmetric and asymmetric fission modes and in the mechanism of sharing excitation energy between fission fragments.

(3) Influence of excitation energy of compound nuclei on the mechanism of charge division between the fission fragments and on odd-even effects in the fission fragment formation probabilities.

The formation cross section of a product with mass number A and charge number Z in fission induced by protons with bombarding energy E_p can be expressed in the form [5]

$$\sigma_{pf}(A,Z,E_p)=\sum_{A_c,Z_c}\int dE_c Y_{\rm post}(A,Z,A_c,Z_c)\frac{d\sigma_{pf}(A_t,Z_t,E_p,A_c,Z_c,E_c)}{dE_c}, \tag{1}$$

where subscripts t and c refer to target and compound nuclei, respectively, $d\sigma_{pf}/dE_c$ is a fission cross section of a compound nucleus at the excitation energy E_c for different fission chances over which the summing is carried out, $Y_{\rm post}$ is an independent yield of the postneutron emission fragments. The partial fission cross sections $d\sigma_{pf}/dE_c$ for the proton bombarding energies up to 30 MeV are calculated in the framework of the cascade evaporating statistical model with accounting preequilibrium neutron emission as in Ref. [28]. The independent fission product yields $Y_{\rm post}$ are formed in the process of neutron emission from the primary fission fragments. The charge distribution of the isobaric chain for the primary fragments is assumed to have Gaussian form with the dispersion approximated by the expression

$$\sigma_Z^2(A,E_c)=0.10+0.025E_c^{1/2}+\delta_{cd},\quad \delta_{cd}=\begin{cases}-0.08, & A \text{ even, } N \text{ even},\\ +0.08, & A \text{ even, } N \text{ odd},\\ -0.04, & A \text{ odd, } N \text{ odd},\\ +0.04, & A \text{ odd, } N \text{ even}.\end{cases} \tag{2}$$

The average charge of a fragment in an isobaric chain is expected to deviate from the unchanged charge density value

$$\bar{Z}(A)=A\frac{Z_c}{A_c}+\delta\bar{Z}(A). \tag{3}$$

The results of Ref. [29] and our calculations of independent fission product cross sections [5] show that even at a few tens MeV of compound nucleus excitation energy the mechanism of charge division differs from the unchanged charge density (UCD) model predictions. Small deviations in $\bar{Z}-\bar{Z}_{\rm UCD}$ values have nearly no influence on the isobaric cumulative yields, but the independent isotopic and charge distributions are very sensitive to these deviations. In these calculations we used the values of $\delta\bar{Z}(A)$ obtained from the fits of the calculated and the experimental independent cross sections [5] and from the independent yields of the isobaric chains with $A=110$, 112, and 114 [1].

The preneutron fragment mass distribution is approximated by the superposition of seven Gaussian distributions:

$$Y_{\rm pre}(A,A_c,Z_c,E_c)=N_s(A_c,Z_c,E_c)y_s(A,A_c,Z_c,E_c)+N_a(A_c,Z_c,E_c,)y_a(A,A_c,Z_c,E_c), \tag{4}$$

where y_s and y_a are symmetric and asymmetric components with weights N_s and N_a, respectively. The asymmetric component is considered as superposition of three components corresponding to different nuclear shells in the fragments:

$$y_a=y_{a1}+Fy_{a2}+Dy_{a3}. \tag{5}$$

Each asymmetric component consists of two Gaussians representing the heavy and light fragment mass groups. The component y_{a1} is connected with the magic numbers $Z=50$ and $N=82$ in the heavy fragments and y_{a3} is influenced by the nuclear shells $Z=28$ and $N=50$ in the light fragments. The asymmetric mode y_{a2} is supposed to be connected with the "deformed" nuclear shell at $N=86$–90. The competition between symmetric and asymmetric fission modes is described by the function R

$$N_s=\frac{200\%R}{1+2R},\quad N_a=\frac{200\%R}{(1+2R)(1+F+D)}. \tag{6}$$

We propose the parametrization of the function R in the spirit of scission point fission model in the form

$$R=\exp\left(-2(\delta U_{a1}+\delta U_{a2}+\delta U_s)\frac{1+\exp(-E_{\rm SC}^{1/2})}{E_{\rm SC}^{1/2}}-1.3E_{\rm SC}^{1/4}\right), \tag{7}$$

where δU_s is a shell correction at the scission point for the average nucleus of symmetric component, δU_{a1} and δU_{ah} are shell corrections at the scission point for the average masses of asymmetric components y_{a1} and y_{a2}, the value $E_{\rm SC}$ is determined by excitation energy at the scission point

$$E_{\rm SC}=E_C+0.03A_C^{2/3}\left(\frac{Z_C^2}{A_C}-26.12\right)-21. \tag{8}$$

The competition between two main asymmetric modes for a wide range of the compound nucleus mass number have been investigated in Ref. [30]. Using the data of this work we approximated the ratio of the light asymmetric component to the heavy one by the relation

$$\frac{1}{F} = \begin{cases} 0.02 + 0.002(A_c - 220)^2 - 0.000\,086\,6(A_c - 220)^3, & A_c \leq 240, \\ 0.19 + 0.0015(A_c - 248)^2, & A_c > 240. \end{cases} \quad (9)$$

The weight of the y_{a3} is small and the function D is approximated by the expression

$$D = F \exp\{0.138(Q_{a3} - Q_{a2})/[(E_{SC} + 20)/0.1A_C]^{1/2}\}, \quad (10)$$

where Q_{a2} and Q_{a3} are Q values for average mass division of second and third asymmetric components.

The prompt neutron multiplicity distribution is assumed to have Gaussian form. A simple approximation for the dispersion of this distribution is written as

$$\sigma_\nu(A, Z, E_C) = 0.75 + 0.21\bar{\nu}(A, Z, E_C), \quad (11)$$

where $\bar{\nu}(A, Z, E_C)$ is the average neutron multiplicity. There are no experimental data for average neutron multiplicities of different members of an isobaric chain. Therefore we used the simple approximation

$$\bar{\nu} = \bar{\nu}(A, E_C) f(A, Z), \quad (12)$$

where f is proportional to the excitation energy of the two fragments and the average value of f for an isobaric chain is equal to unity.

The average prompt fission neutron multiplicities $\bar{\nu}(A, E_C)$ were calculated in the framework of the simple scission point fission model. The scission point configuration is approximated by two tangential spheroid-shaped fragments with a distance between the tips of the fragments d. The fragment deformation parameters are determined from the condition of minimum of the potential energy at the scission point

$$V = V_{\text{Coul}} + E^l_{\text{def}} + E^h_{\text{def}}, \quad (13)$$

where V_{Coul} is the Coulomb interaction energy between the fragments. E^l_{def} and E^h_{def} are the deformation energies of the light and the heavy fragments calculated according to the relations

$$E_{\text{def}} = \alpha(b - R_0)^2, \quad R_0 = r_0 A^{1/3}, \quad r_0 = 1.35 \text{ fm}, \quad (14)$$

where b is the large semiaxis of a deformed fragment. The stiffness coefficient α depends on the shell correction δU and temperature according to the formula

$$\alpha = \alpha_{\text{LDM}}(K - \delta U)/(K + \delta U), \quad (15)$$

where K is a constant. The temperature dependence of shell corrections is described by the relation given in Ref. [31] as follows

$$\delta U = \delta U(0) t^2 \cosh t/(\sinh^2 t), \quad t = 2\pi^2 T/(41 A^{-1/3}), \quad (16)$$

where T is temperature at the scission point. The stiffness coefficient in the liquid drop model approximation is equal to

$$\alpha_{\text{LDM}} = (0.16\pi/r_0^2)[a_2(1 - k_s(N - Z)^2/A^2) - \tfrac{1}{2}c_3 Z^2/A]. \quad (17)$$

The average excitation energy of fragments is determined by the deformation energy and the thermal energy at the scission point E^*_{SC}

$$\bar{E}^* = \bar{E}^*_{SC} + E_{\text{def}}. \quad (18)$$

The total thermal energy at the scission point is divided between fragments according to the thermal equilibrium condition. The level density parameters are calculated using the systematics of Ref. [32]. The average prompt fission neutron multiplicities are calculated using the simplified evaporation model. In these calculations we used the constants

$$K = 8 \text{ MeV}, \quad k_s = 0.79, \quad a_2 = 18.56 \text{ MeV}, \quad c_3 = 0.717 \text{ MeV}, \quad d = 2 \text{ fm}. \quad (19)$$

To avoid the calculations of the shell corrections at scission point in the macro-microscopic model we used a phenomenological procedure. Using experimental data of average neutron multiplicities in the spontaneous fission of ^{252}Cf and thermal neutron fission of ^{235}U the shell corrections at the scission point have been determined. The linear interpolation relative to the compound nucleus mass number between these reference shell corrections is used to obtain the shell corrections of fragments at scission point in fission of other compound nuclei.

VI. DISCUSSION

Using the measurements of the cumulative yields the mass yield curve has been obtained for the symmetric fission, for which earlier information was practically nonexistent. Comparison of the experimental data and the calculated mass yield curve for the fission of ^{238}U induced by 19.8 MeV protons is shown in Fig. 3, where the theoretical cross section scale has been adjusted to the overall experimental efficiency. We have used the independent yields of Tc isotopes for scaling the total experimental and the calculated isotopic yields to get a correspondence factor of 0.048 43 mb/(atoms/μC) between the yield and the cross section. The total sum is not biased by other parameters describing a distribution. We can see a good agreement between the experimental and calculated cumulative yields in the symmetric mass region. In the case of earlier gamma-spectroscopy measurements [5] the experimental points were systematically higher in symmetric mass region than the calculated ones. Differences for $A = 119$ and 120 can be removed by adding the independent yields of elements Cd and In. A more complex

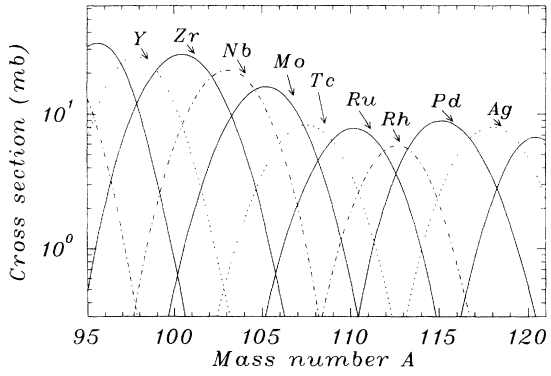

FIG. 4. Independent isotope distributions from Y to Ag as calculated with the model described in the text.

TABLE II. Calculated parameters of the independent isotopic fission product distributions $\bar{A}$, σ_A, b_A in the reaction 19.8 MeV p+^{238}U.

Z	$\bar{A}(Z)$	$\sigma_A(Z)$	$b_A(Z)$
38	95.41	1.72	−0.08
39	97.87	1.74	0.06
40	100.44	1.95	0.04
41	103.02	1.85	−0.07
42	105.14	1.91	−0.05
43	107.49	1.94	0.10
44	110.12	1.91	−0.11
45	112.61	1.75	0.07
46	115.28	1.93	0.13
47	117.91	1.85	−0.08

experimental problem is the case of elements Y and Nb, for which the oxide yields should be estimated more accurately. Results of Refs. [4,5] show higher yields for $A = 111$–113 relative to a smooth curve indicating some kind of structure. However, our results do not support this observation.

Independent isotopic fission product distributions in the near symmetric mass region have been measured for the first time. In this work they can be derived for Tc, Ru, and Rh using the cumulative yields given in Table I. These data are very important for testing the following aspects of fission theories: competition of different fission modes, charge division, odd-even effects, and mechanism of sharing excitation energy between fragments. The calculated independent isotopic distributions for $Z = 40$–47 are shown in Fig. 4 and their comparison with the experimental values for Tc, Ru, and Rh are shown in Fig. 5. It can be seen that these distributions have approximately a Gaussian form but in the mass region on the right-hand slope of the light asymmetric mass peak the model isotopic distributions differ from Gaussian form showing asymmetric behavior. There are discrepancies between the theoretical and experimental independent fission product distributions. For element Tc the calculated cross sections exceed experimental ones on the neutron-rich side. In the case of element Rh the experimental and theoretical distributions are in satisfactory

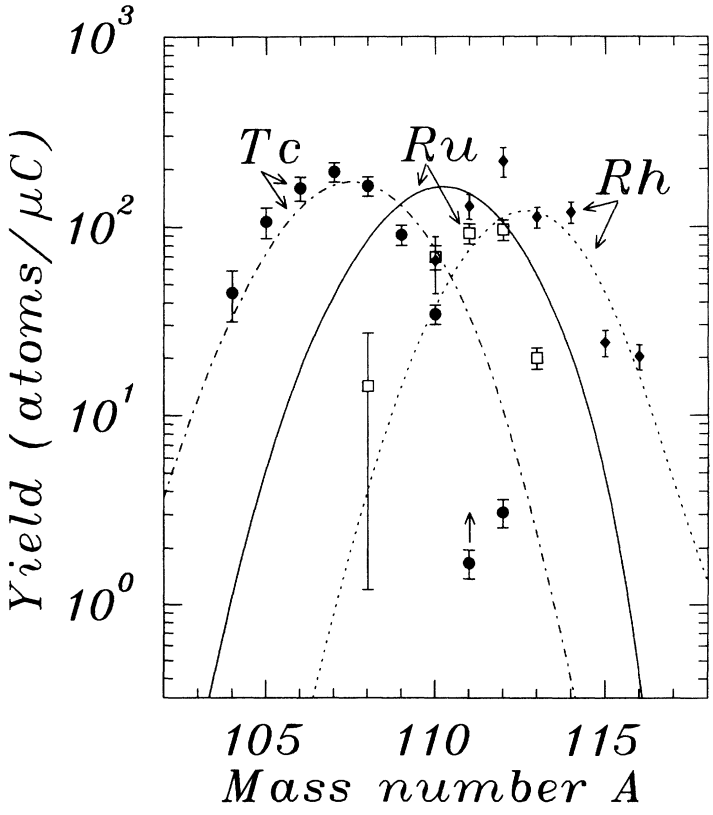

FIG. 5. Comparison of the calculated and the measured independent isotope distributions for Tc, Ru, and Rh. The experimental values have been extracted from Table I in Sec. IV.

TABLE III. Deviation $\delta\bar{Z} = \bar{Z} - \bar{Z}_{\rm UCD}$ for the preneutron emission isobaric chains for the fissioning compound nucleus ^{239}Np produced in the proton bombardment of ^{238}U.

A	96	97	98	99	100	101	102	103	104	105
$\delta\bar{Z}$	0.05	−0.05	−0.10	−0.15	−0.10	−0.15	−0.20	−0.30	−0.40	−0.45
A	106	107	108	109	110	111	112	113	114	115
$\delta\bar{Z}$	−0.45	−0.50	−0.60	−0.55	−0.60	−0.45	−0.40	−0.40	−0.35	−0.35
A	116	117	118	119	120					
$\delta\bar{Z}$	0.10	0.25	0.30	0.15	−0.15					

agreement. The experimental points for Rh show an odd-even effect that is not reproduced by the theoretical model. It is worthwhile to emphasize that in Fig. 5 the same scaling factor as in Fig. 3 is used. The large discrepancy between the theoretical and experimental distributions for element Ru is not presently understood.

Deviation from the symmetric distribution can be described by an asymmetry parameter

$$b_A = \frac{\sum(A_i - \bar{A})^3 Y_i}{\sigma_A^3 \sum Y_i}, \tag{20}$$

where A_i and Y_i are the appropriate mass number and the corresponding fission product yield and σ_A is the dispersion of the distribution. The parameters of the calculated isotopic distributions A, σ_A, and b_A are given in Table II. The dependence of $\bar{A}$ on the atomic number Z can be approximated by the relation

$$\bar{A}(Z) = Z(A_c - \nu_{\rm tot})/Z_c + \delta\bar{A}(\bar{Z}), \tag{21}$$

where A_c and Z_c are the mass and the charge of the composite system in the entrance channel and δ is a deviation from the linear dependence and is connected with the shell structure. Using the calculated cumulative mass distribution we can estimate an average neutron multiplicity $\nu_{\rm tot} = A_c - (\bar{A}_L + \bar{A}_H)$, where $\bar{A}_L$ and $\bar{A}_H$ are the average masses of the light and the heavy mass peaks. In the present case $\bar{A}_L = 135.29$, $\bar{A}_H = 98.28$, and $\nu_{\rm tot} = 5.43$. To describe the experimental data of independent fission product formation cross sections presented in this and earlier works [1,5], it is necessary to assume that the average charges of the preneutron emission isobaric chain differ from the unchanged charge division. In Table III we present the deviations [see formula (3)] for the compound nucleus ^{239}Np made in the proton-induced fission of ^{238}U. From this comparison we see that charge division between fragments differs from the unchanged charge division in fission of heavy nuclei at excitation energy up to 25 MeV and that the dependence of $\delta Z(A)$ is influenced by the nearby shell at $Z = 50$.

VII. CONCLUSION

Cumulative and independent product yields in the near symmetric mass region in 20 MeV proton induced fission of ^{238}U were measured by the on-line mass separator IGISOL for the first time. The theoretical model to calculate product mass and isotope distributions is described. A comparison of theoretical and experimental yields shows that the theoretical model may be used for evaluation of fission product yields and predictions of the production rates of very neutron-rich nuclei in the light particle induced fission. It was found that the mechanism of charge splitting at scission point is influenced by nuclear shells at the compound nucleus excitation energy up to a few tens of MeV. The on-line mass separator IGISOL can be used successfully for investigation of shell and pairing effects in charge and isotopic distributions in fission in the symmetric and very asymmetric mass regions. We intend to continue our studies of isotopic product distribution and charge distribution using the new heavy ion cyclotron in Jyväskylä. Different light and heavy ions are available also at higher energies than in this work and enable the study of, e.g., the effect of the excitation energy on the fission properties.

This work was supported by the Academy of Finland and the Committee on Scientific and Technical Co-Operation Program between Finland and Russia.

[1] M. Leino, P. P. Jauho, J. Äystö, P. Decrock, P. Dendooven, K. Eskola, M. Huyse, A. Jokinen, J. M. Parmonen, H. Penttilä, G. Reusen, P. Taskinen, P. Van Duppen, and J. Wauters, Phys. Rev. C **44**, 336 (1991).

[2] W.-D. Schmitt-Ott, F. Meissner, P. Koschell, U. Bosch-Wicke, R. Kirchner, O. Klepper, H. Folger, E. Roeckl, A. Plochocki, K. Rykaczewski, and Z. Preibisz, Nucl. Phys. **A522**, 610 (1991).

[3] A. Astier, R. Béraud, A. Bouldjedri, R. Duffait, A. Emsallem, M. Meyer, S. Morier, P. Pangaud, N. Redon, D. Barnéoud, J. Blachot, J. Genevey, A. Gizon, R. Guglielmini, J. Inchaouh, G. Margotton, J. L. Vieux-Rochaz, J. Ärje, J. Äystö, P. Jauho, A. Jokinen, H. Penttilä, K. Eskola, M. E. Leino, and J. B. Marquette, Nucl. Instrum. Methods **70**, 233 (1992).

[4] T. Ohtsuki, Y. Nagame, K. Tsukada, N. Shinohara, S. Baba, K. Hashimoto, I. Nishinaka, K. Sueki, Y. Hatsukawa, K. Hata, T. Sekine, I. Kanno, H. Ikezoe, and H. Nakahara, Phys. Rev. C **44**, 1405 (1991).

[5] E. Karttunen, M. Brenner, V. A. Rubchena, S. A.

Egorov, V. B. Funschtein, V. A. Jakovlev, and Yu.A. Selitskiy, Nucl. Sci. Engin. **109**, 350 (1991).
[6] R. Vandenbosch and J. R. Huizenga, *Nuclear Fission* (Academic, New York, 1973).
[7] J. Ärje, J. Äystö, P. Taskinen, J. Honkanen, and K. Valli, Nucl. Instrum. Methods **26**, 384 (1987).
[8] P. Taskinen, H. Penttilä, J. Äystö, P. Dendooven, P. Jauho, A. Jokinen, and M. Yoshii, Nucl. Instrum. Methods **281**, 539 (1989).
[9] G. Lhersonneau, Nucl. Instrum. Methods **157**, 349 (1978).
[10] M. Strecker, R. Wien, P. Plischke, and W. Scobel, Phys. Rev. C **41**, 2172 (1990).
[11] L. C. Northcliffe and R. F. Schilling, Nucl. Data Tables A **7**, 233 (1970).
[12] J. F. Ziegler, J. P. Biersack, and U. Littmark, *The Stopping and Ranges of Ions in Solids* (Pergamon, New York, 1985).
[13] H. Kudo, Y. Nagame, and H. Nakahara, K. Miyano, and I. Kohno, Phys. Rev. C **25**, 909 (1982).
[14] J. Äystö, P. Taskinen, M. Yoshii, J. Honkanen, P. Jauho, H. Penttilä, and C. N. Davids, Phys. Lett. B **201**, 211 (1988).
[15] J. Äystö, C. N. Davids, J. Hattula, J. Honkanen, K. Honkanen, P. Jauho, R. Julin, S. Juutinen, J. Kumpulainen, T. Lönnroth, A. Pakkanen, A. Passoja, H. Penttilä, P. Taskinen, E. Verho, A. Virtanen, and M. Yoshii, Nucl Phys. **A480**, 104 (1988).
[16] H. Penttilä, P. Taskinen, P. Jauho, V. Koponen, C. Davids, and J. Äystö, Phys. Rev. C **38**, 931 (1988).
[17] V. Koponen, J. Äystö, C. Davids, J. Honkanen, P. Jauho, H. Penttilä, K. Rykaczewski, P. Taskinen, and J. Zylicz, Z. Phys. A **333**, 339 (1989).
[18] H. Penttilä, J. Äystö, P. Jauho, A. Jokinen, J. Parmonen, P. Taskinen, K. Eskola, M Leino, P. Dendooven, and C. Davids, Phys. Scr. **T32**, 38 (1990).
[19] J. Äystö, P. Jauho, Z. Janas, A. Jokinen, J. Parmonen, H. Penttilä, P. Taskinen, R. Beraud, R. Duffait, A. Emsallem, J. Meyer, M. Meyer, N. Redon, M. Leino, K. Eskola, and P. Dendooven, Nucl. Phys. **A515**, 365 (1990).
[20] H. Penttilä, J. Äystö, Z. Janas, P. Jauho, A. Jokinen, M. Leino, J. Parmonen, and P. Taskinen, Z. Phys. A **338**, 291 (1991).
[21] H. Penttilä, P. Jauho, J. Äystö, P. Decrock, P. Dendooven, M. Huyse, P. Van Duppen, and J. Wauters, Phys. Rev. C **44**, 935 (1991).
[22] A. Jokinen, J. Äystö, P. Dendooven, K. Eskola, Z. Janas, P. Jauho, M. Leino, J. Parmonen, H. Penttilä, K. Rykaczewski, and P. Taskinen, Z. Phys. A **340**, 21 (1991).
[23] J. Äystö, A. Astier, T. Enqvist, K. Eskola, Z. Janas, A. Jokinen, K.-L. Kratz, M. Leino, H. Penttilä, B. Pfeiffer, and J. Zylicz, Phys. Rev. Lett. **69**, 1167 (1992).
[24] A. Jokinen, J. Äystö, K. Eskola, Z. Janas, P. Jauho, M. Leino, J. Parmonen, and H. Penttilä, Nucl. Phys. **A549**, 420 (1992).
[25] Z. Janas, J. Äystö, K. Eskola, J. Kownacki, M. Leino, P. Jauho, A. Jokinen, J. Parmonen, H. Penttilä, J. Szerypo, and J. Zylicz, Nucl. Phys. **A552**, 340 (1993).
[26] H. Penttilä, T. Enqvist, P. Jauho, A. Jokinen, M. Leino, J. Parmonen, J. Äystö, and K. Eskola, Nucl. Phys. **A561**, 416 (1993).
[27] G. Lhersonneau, K.-L. Kratz, B. Pfeiffer, J. Äystö, T. Enqvist, P. Jauho, A. Jokinen, J. Kantele, M. Leino, J. Parmonen, and H. Penttilä, Phys. Rev. C **49**, 1379 (1994).
[28] V. A. Ageev, S. A. Egorov, V. Ya. Golovnya, E. A. Gromova, S. S. Kovalenko, A. F. Linev, Yu. A. Nemilov, A. V. Pozdnyakov, V. A. Rubchenya, Yu. A. Selitsky, A. M. Fridkin, and V. A. Yakovlev, Yad. Fiz. **46**, 1200 (1987) [Sov. J. Nucl. Phys. **46**, 700 (1987)].
[29] B. L. Tracy, J. Chaumont, R. Klapisch, J. M. Nitschke, A. M. Poskanzer, E. Roeckl, and C. Thibauldt, Phys. Rev. C **5**, 222 (1972).
[30] M. G. Itkis and V. N. Okolovich, in "Dynamical Aspects of Nuclear Fission," Proceedings of the International Workshop, June 17–21, 1991, Smolenice, edited by J. Kristiak and B. I. Pustylnik (in press), p. 226.
[31] A. Bohr and B. Mottelson, *Nuclear Structure* (Benjamin, New York, Amsterdam, 1969).
[32] A. V. Ignatyuk *et al.*, Yad. Fiz. **29**, 875 (1979) [Sov. J. Nucl. Phys. **29**, 450 (1979)].